Local Polarity and Microviscosity in the Hydrophobic Cores of Amphiphilic Star-like and Scorpion-like Macromolecules

Karen E. Steege, Jinzhong Wang, Kathryn E. Uhrich,* and Edward W. Castner, Jr.*

Department of Chemistry and Chemical Biology Rutgers, The State University of New Jersey, 610 Taylor Road, Piscataway, New Jersey 08854-8087

Received August 4, 2006; Revised Manuscript Received March 16, 2007

ABSTRACT: Fluorescence spectroscopy is used to probe the polarity and local friction in aqueous solutions of three amphiphilic polymers. Aggregate core polarity and local friction on the nanoscale are observed by measuring the steady-state and time-resolved fluorescence spectroscopy of coumarin 153 (C153) in three amphiphilic polymers as a model for hydrophobic drug encapsulation. Three solutions of polymers are studied: one amphiphilic scorpion-like macromolecule (AScM), M12P5, and two amphiphilic star-like macromolecules (ASMs), NC12P5 and NC6P5. Both ASMs and AScMs consist of hydrophobic segments of acylated mucic acid and hydrophilic poly(ethylene glycol) chains. In aqueous solution, the scorpion-like M12P5 forms micellar aggregates through hydrophobic interactions, while the star-like polymers are covalently bonded macromolecules that form higher order aggregates. Micelle and aggregate sizes are compared using dynamic light scattering measurements. A shift in the steady-state emission wavelength of C153 indicates distinct differences in polarity between the core environments of the scorpion-like polymer micelles and those of the two star-like polymers. The two reorientation time constants from C153 fluorescence anisotropies show that the hydrophobic cores of M12P5 micelles are relatively flexible. The covalently linked, rigid cores of the two star-like macromolecule nanocarriers, NC6P5 and NC12P5, show a third reorientation time constant for which the local friction of the dye is remarkably higher.

Introduction

A number of amphiphilic polymers have been designed to solubilize hydrophobic molecules for applications in drug delivery.[1−4] Because poly(ethylene glycol) (PEG) is highly water-soluble, it is ubiquitous in these synthetic copolymers.[5] PEG and its conjugates are widely used in the areas of small-molecule encapsulation, drug formulation, modification of proteins and pharmaceutical molecules, cosmetics, biomedical coatings, and other surface modifications.[1−6] The hydrophilic, nontoxic, biocompatible, and biodegradable nature of PEG has led to its use in amphiphilic polymers for encapsulation of hydrophobic drugs.[1,2] Many molecules considered as drug candidates are insufficiently water-soluble to be absorbed effectively into biological systems, and one must take into account the solubility and biological interactions of both the drug and its delivery media.[2] Such delivery media must be biocompatible, nontoxic, and able to solubilize but not inhibit the drug molecule. Each of these attributes depends on appropriate selection of the PEG functionality.[2,5,7,8] Another goal of drug delivery systems is to simultaneously increase the circulation time while decreasing the dosage.[1] This can enable a reduction of cytotoxicity, such as for chemotherapy drugs.[1]

Amphiphilic polymers with PEG hydrophilic blocks have been used for increased solubility of hydrophobic molecules.[1−4] Here, we examine three such amphiphilic polymers with the coumarin 153 (C153) fluorescence probe encapsulated as a reporter of local environment within the core of each of three polymer solutions. C153 is used as a hydrophobic drug model for observation of the local friction and local solvent polarity in the core of each nanocarrier.[9−13]

C153 is a well-characterized solvatochromic fluorescence probe that has a hydrophobic *clogP* value of 4.08.[14] The structure of C153 is shown in Figure 1. This extrinsic fluorophore has a broad absorption peak near 425 nm. The emission

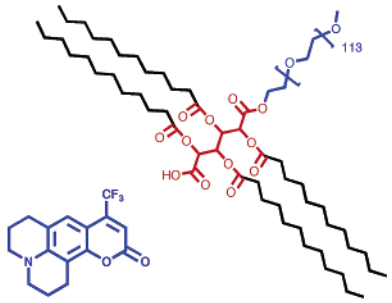

Figure 1. Structure of fluorescence dye C153 (left) and amphiphilic scorpion-like macromolecule, M12P5 (right).

maximum ranges from 450 nm in a nonpolar solvent such as perfluorohexane to 567 nm in a polar solvent such as ethylene glycol.[9,15,16] The ability to probe the local solvent environment of C153 has been used previously by our group to investigate the local polarity and microviscosity in different regions of aqueous solutions of poly(ethylene oxide)−poly(propylene oxide)−poly(ethylene oxide) triblock copolymers.[17,18] By measuring the steady-state fluorescence emission, time-dependent polarization anisotropy, and reorientation time constants of C153, it is possible to clearly distinguish between a flexible, polar, water-like environment and a more rigid, nonpolar environment of the dye molecule.[17,19]

In the following, C153 is solubilized by three different amphiphilic polymers designed for encapsulation of hydrophobic drugs. The first of the three polymers is an amphiphilic scorpion-like macromolecule (AScM) composed of a hydrophilic, methoxy-terminated PEG tail of molecular weight 5000 g/mol and a hydrophobic constituent consisting of acylated mucic acid with 12 aliphatic carbons on each of four ester groups.[20] This polymer is called M12P5 and is shown in Figure 1.[21] M12P5 forms micelles in aqueous solution with a cmc of 1.25×10^{-7} mol/L at room temperature.[20]

10.1021/ma061779l CCC: $37.00
Published on Web 04/18/2007

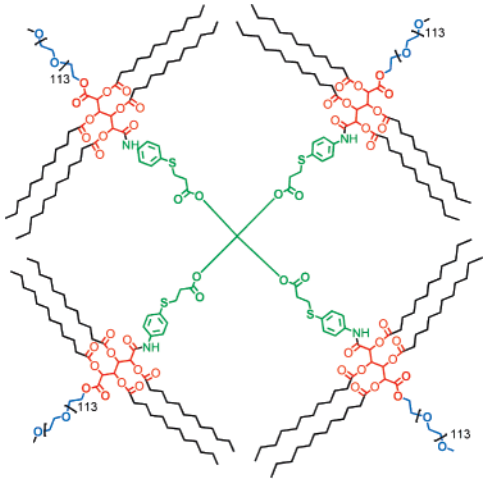

Figure 2. Structure of amphiphilic star-like macromolecule, NC12P5.

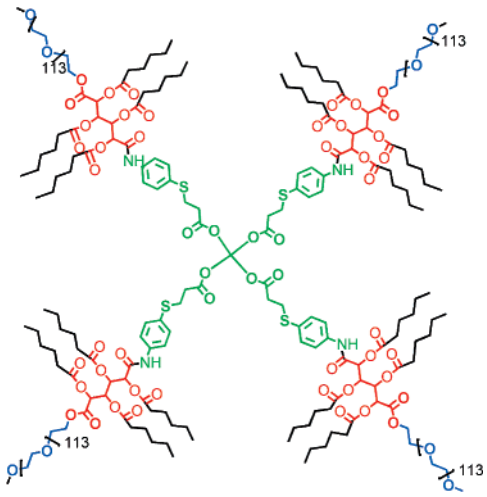

Figure 3. Structure of amphiphilic star-like macromolecule, NC6P5.

The second drug-delivery polymer shown in Figure 2 is called NC12P5 and is one of two amphiphilic star-like macromolecules (ASMs).[22,23] Like M12P5, NC12P5 has a hydrophilic PEG (M_w 5000 g/mol) tail attached to the acylated mucic acid core.[22] Unlike an AScM, NC12P5 has four amphiphilic branches covalently joined in the center to form a single star-like macromolecule that behaves like a "unimolecular micelle".[22,23] The third polymer is another ASM called NC6P5 and differs from NC12P5 by having only six carbon chains on each of the four mucic acid acylation sites.[23] The structure of NC6P5 is shown in Figure 3.[23] Both the two ASM molecules and the AScM molecule that we have studied here have methoxy-terminated PEG chains.[20,23]

The difference in hydrophobic cores between the star-like macromolecules and the scorpion-like macromolecules leads to questions about the resulting structures, the size scales, and the aggregation properties of each of the polymers in aqueous solution. M12P5 scorpion-like macromolecules aggregate in water to form spherical micelles, as seen by transmission electron microscopy (TEM) in a previous study.[23,24] In the case of the TEM study, the images taken were done in vacuum, with samples prepared by freeze-fracture methods.[23,24] In this study, we use dynamic light scattering to measure particle size distributions of each of the three polymers in solution.

The volume for each polymeric unimer is estimated from incremental van der Waals calculations.[25,26] The volume of each aggregate obtained from analysis of the DLS data can then be compared to the volume of a single unimer and to the effective volume of coumarin 153 reorientation found from time-resolved fluorescence anisotropy measurements. This last effective volume provides insight into the local friction felt by an encapsulated hydrophobic molecule in each of the three nanocarriers in question. This local friction is relevant to the capacity for each polymeric nanocarrier to encapsulate and release hydrophobic molecules in solution.

The local friction experienced by C153 solvated in each nanocarrier differs from the bulk viscosity of these dilute solutions. As shown by Horng et al., the reorientation of a polar molecule such as C153 is governed by dielectric friction with its surrounding solvent environments of various polarities.[10] This friction strays from typical hydrodynamic theory in many cases, thus causing a difference in macroscopic and nanoscale viscosities.[10,27]

The purpose of the following study is to use C153 fluorescence to characterize the local environment in the core of each drug-delivery polymer. Properties of the C153 local environment such as solvent polarity, microviscosity, and effective size serve as a model for probing the core environment of an encapsulated drug molecule.[17−19] By revealing the nature of the local environment inside each nanocarrier, the polarity and flexibility of each drug delivery vehicle may be compared relative to each other for the purpose of encapsulating a hydrophobic molecule. The aggregation properties and size scales are explored by dynamic light scattering, by van der Waals molecular volume calculations, and by investigating the fluorescence and reorientation of C153 inside each polymer solution.

Materials and Methods

Sample Preparation. NC12P5 and NC6P5 amphiphilic star-like macromolecules (ASMs) and the M12P5 amphiphilic scorpion-like macromolecule (AScM) were synthesized and purified according to the previously published procedures.[20,22] Aqueous solutions of each of the three polymers were prepared using Fluka Nanopure water and stirred in the dark at room temperature for at least 48 h. The polymer solutions were filtered through a 0.2 μm Whatman PTFE filter to remove impurities. Molar concentrations for these three solutions are 2×10^{-4} mol/L for M12P5, 5×10^{-5} mol/L for NC12P5, and 5×10^{-5} mol/L for NC6P5, giving all solutions approximately the same weight-to-volume ratio of 1.2 to 1.3 g/L. The concentration of M12P5 solution is well above the cmc value of 1.25×10^{-7} mol/L.[20] Solid coumarin 153 (C153) from Acros Organics was added to each polymer solution in a sealed vial and stirred for at least 24 h until dissolved into solution.

The aggregation properties of ASMs and AScMs depend on the concentration of each polymer in solution. For all of the fluorescence measurements reported here, we have used polymer concentrations above the critical aggregation concentration for each of the measurement temperatures. For the present fluorescence experiments, we have not studied any ASM or AScM solutions at unimer concentrations, only at higher concentrations for which our DLS results prove the presence of higher-order aggregates.

The polymer concentrations for each set of fluorescence experiments were selected using several criteria. First, only at higher concentrations of polymer can we avoid more than a single C153 fluorescence probe per polymer aggregate, as lower concentrations reduce the optical signals to unacceptable levels. Second, the goal of our work was to study aggregates and micelles of the ASM and AScM polymers in aqueous solution, since these are the relevant target size for good bioavailability and drug encapsulation purposes.

Dynamic Light Scattering (DLS). A Nicomp 380 submicron particle sizing system with drop-in sample loading and a 532 nm laser was used for particle size analysis of all polymer solutions. For DLS studies at 37 °C, polymer concentrations ranged from 1×10^{-3} to 1×10^{-9} mol/L. Temperature-dependent DLS studies between 5 and 55 °C were done using polymer concentrations of

2×10^{-4} mol/L for M12P5 and 5×10^{-5} mol/L for both NC12P5 and NC6P5. Nicomp volume-weighted distributions are used for determination of polymer aggregate sizes. Before measurement, all solutions were centrifuged and filtered through 0.2 μm syringe filters. All samples were allowed to equilibrate at the temperature set point for at least 10 min before measurement.

Viscosities. A Cambridge Applied Systems model ViscoLab 4100 automated viscometer was used for all viscosity measurements. A Lauda Brinkmann RMT-6 recirculating chiller provided temperature control of ±0.1 °C. Each of the three polymer solutions was held at each temperature for at least 15 min for proper equilibration. A steel piston of 0.310 in. diameter was selected to measure viscosities in the range 0.25−5 cP for all polymer solutions.

Steady-State Emission and Excitation Spectra. Steady-state fluorescence emission and excitation spectra of C153 in each solution were measured with a Spex Fluoromax-3 fluorometer with 425 nm excitation and 510 and 530 nm emission wavelengths for ASMs and AScM samples, respectively. Calcite polarizers were used in the spectrophotometer for steady-state anisotropy measurements. The temperature of the sample was controlled using a Wavelength Electronics thermoelectric temperature controller to ±0.1 °C. Sample equilibration time at each temperature was 10 min. To determine the peak wavelength, the steady-state spectra were graphed, and the full width of the intensity at 90% the peak maximum was fit to a Gaussian line shape with Igor software from Wavemetrics.[28]

Time-Resolved Fluorescence. The time-correlated single photon counting (TCSPC) apparatus was previously described in detail.[17,29−31] Samples were excited at 425 nm. A 70 ns time window having 4096 data points was used. The measured instrument temporal response was typically 80 ps at full width half-maximum. The C153 emission decay transients were detected at 510 nm for NC12P5 and NC6P5 polymer samples and 530 nm for M12P5 polymer samples. Sample temperatures were controlled to ±0.1 °C using a Quantum Northwest TLC 50/100 thermoelectric temperature controller with 10 min thermal equilibration times.

Time-resolved emission decay transients at vertical (VV), magic (VM), and horizontal (VH) polarization angles of detection were simultaneously fit using Igor software[28] by a generalization of the simultaneous VV and VH transient fitting described by Cross and Fleming.[32] Equations 1−5 were used for simultaneous fitting of the three decays. Equations 1 and 2 for $K(t)$ and $I_{VM}(t)$ represent the fit to the emission decay transient measured at magic angle polarization, where the α_i are the normalized amplitudes that sum to unity and the τ_i are the component time constants.

$$K(t) = \sum_{i=1}^{n} \alpha_i \exp\left(\frac{-t}{\tau_i}\right) \tag{1}$$

$$I_{VM}(t) = K(t) \tag{2}$$

The emission decay transients measured at vertical and horizontal polarization angles are fit to eqs 3 and 4, respectively, and these are functions of $K(t)$ and $r(t)$, where $r(t)$ is the time-resolved decay of polarization anisotropy, r_j are amplitudes that sum to the fundamental anisotropy, and $\theta_{j,rot}$ are the component reorientation time constants.[32−34]

$$I_{VV} = \frac{1}{3}K(t)(1 + 2r(t)) \tag{3}$$

$$I_{VH} = \frac{1}{3}K(t)(1 - r(t)) \tag{4}$$

Fits to a multiexponential model for the VM fluorescence decay rates were combined with a multiexponential anisotropy decay law, given in eq 5.[18,32] This fitting was done to calculate fluorescence decay rates and amplitudes as well as reorientation rates and amplitudes. The emission transients, $I_{VV}(t)$, $I_{VM}(t)$, and $I_{VH}(t)$, are shown concatenated in Figure 4 with the reduced residuals from the simultaneous fit.

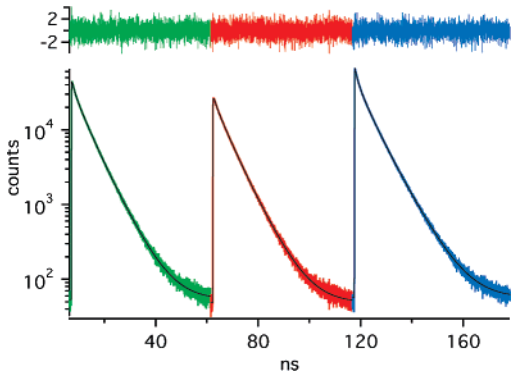

Figure 4. Time-resolved decay transients of C153 emission in 5×10^{-5} mol/L solution of NC6P5 at 20 °C at magic (green), horizontal (red), and vertical (blue) angles of polarization ($I_{VM}(t)$, $I_{VH}(t)$, and $I_{VV}(t)$). Reduced residuals are plotted at the top.

$$r(t) = \sum_{j=1}^{n} r_j \exp\left(\frac{-t}{\theta_{j,rot}}\right) \tag{5}$$

The value of the $\chi^2_{reduced}$ ranged between 1.02 and 1.14 for the nonlinear least-squares fits of the data to eqs 1−5. Simulations of time-resolved fluorescence data made using the experimental data parameters were fit to establish the robustness of the fitting method. Time-resolved emission decays were measured at five temperatures (5, 20, 37, 55, and 70 °C) to obtain a range of reorientation data in different conditions corresponding to refrigeration, room temperature, body temperature, and a heated environment. The range of temperatures also permits variation of the rigidity of the polymer cores due to thermal motion of both the polymer and water. While the window for the time-resolved fluorescence decays of C153 is 70 ns in this case, correct parameters were recovered from simulated data with given longer reorientation time constants beyond this window. Using simulated data sets, reorientation time constants as long as 250 ns can be retrieved accurately from simulated data using our simultaneous fitting method. While the error in accurately obtaining the longer reorientation time constants was greater than obtaining the faster rates within the window of measurement, the error was well within the range of the original calculations.

Results and Discussion

Dynamic Light Scattering. Particle size dependence on polymer concentration and temperature was characterized by DLS. Hydrodynamic radii were obtained from the DLS diffusion coefficients assuming Stokes−Einstein hydrodynamics.[26,34] The Stokes−Einstein equation (eq 6) relates the translational diffusion coefficients (D_0) to the hydrodynamic radii (R_H), where T is the absolute temperature, k_B is the Boltzmann constant, and η is the solvent viscosity.[26,34]

$$D_0 = \frac{k_B T}{6\pi\eta R_H} \tag{6}$$

Particle diameters were measured for aqueous solutions ranging in polymer concentration from 1×10^{-9} to 1×10^{-3} mol/L. Figure 5 shows the volume-weighted distribution of particle diameters found for all three polymer solutions at 37 °C at the same concentrations used for fluorescence experiments. The polymer aggregate diameters obtained from DLS data at 37 °C are plotted vs concentration in the top graph of Figure 6. These data indicate that aggregates begin to form in each of the three polymer solutions, as the concentration approaches 1×10^{-6} mol/L, and that the polymers exist as

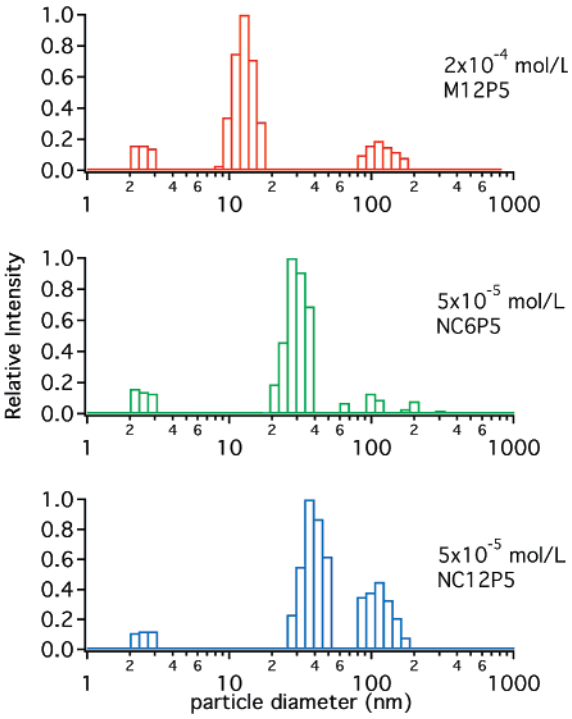

Figure 5. Volume-weighted particle size distributions of M12P5, NC12P5, and NC6P5 polymer solutions at 37 °C, obtained from DLS data.

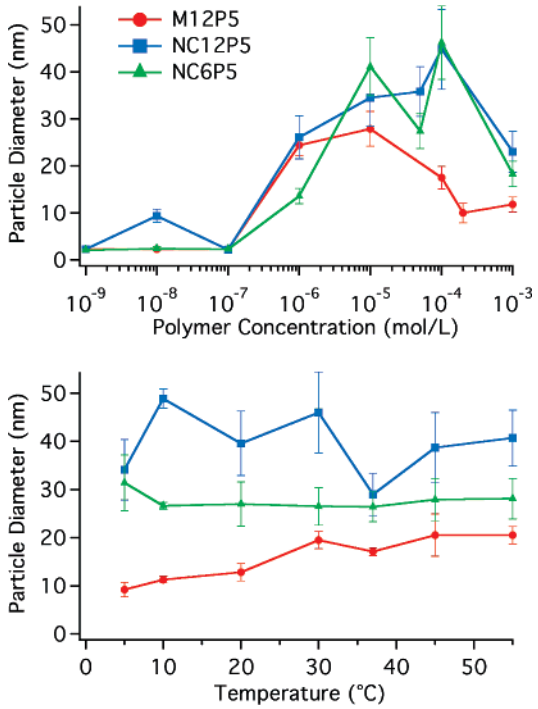

Figure 6. Particle diameters from DLS data vs concentration (top) at 37 °C and vs temperature (bottom) at 2×10^{-4} mol/L of M12P5 and 5×10^{-5} mol/L of both NC12P5 and NC6P5 polymer solutions.

unimers in solution below 100 nM concentration. For concentrations in the range from 1×10^{-7} to 1×10^{-6} mol/L, micellar aggregates are formed. On increasing polymer concentration, the M12P5 aggregates increase and then decrease in size, ranging from 10 to 28 nm in diameter.

The NC12P5 and NC6P5 ASM polymers form larger aggregates at approximately the same polymer concentration. The star-like NC12P5 forms aggregates ranging in diameter from 23 to 45 nm. The other star-like macromolecule NC6P5 forms

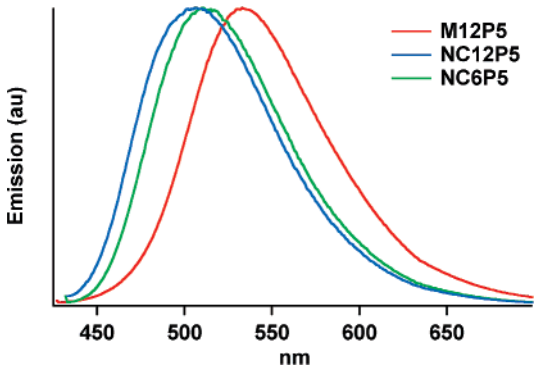

Figure 7. Steady-state emission spectra of C153 in aqueous solutions of M12P5, NC12P5, and NC6P5 solutions at 37 °C.

aggregates ranging in diameter from 14 to 47 nm over the same concentration range. NC6P5 aggregates are smaller compared to the NC12P5 aggregates due to the smaller number of aliphatic carbons present in the NC6P5 molecule. The lower bound for hydrodynamic radii obtained from the analysis of DLS data is ~1 nm for both ASMs and AScMs. This radius is consistent with the size estimated for ASM and AScM unimers.

For comparison with fluorescence experiments, the temperature dependence of particle size for all three polymer solutions was measured at the same concentrations used for fluorescence samples. In the range of 5−55 °C, M12P5 aggregates are trimodal, with unimers, micelles, and larger aggregates present at ~100 nm diameters. The micellar aggregates, which are dominant in solution, have a diameter of 9 nm at 5 °C. The diameters increase to 21 nm at 55 °C. NC12P5 and NC6P5 also display trimodal particle size distributions. The dominant diameter of NC12P5 aggregates is 40 nm. NC6P5 aggregates have an average diameter of 28 nm over the same temperature range. The average diameter of NC12P5 aggregates is larger than the aggregates of NC6P5 due to the greater number of hydrocarbons in the hydrophobic core of the NC12P5 molecule. Again, a small population of larger aggregates are also present around 100 nm particle sizes. The temperature dependence of the dominant aggregate diameters is shown in Figure 6 for all three polymer aggregates. The particle size distribution of each polymer solution at the concentrations of 2×10^{-4} mol/L M12P5, 5×10^{-5} mol/L NC12P5, and 5×10^{-5} mol/L NC6P5 showed relatively little change with increasing temperature. Details of the polymer particle size distributions are provided in the Supporting Information.

Viscosities. The shear viscosity of each of the three polymer solutions at high concentration (1×10^{-3} mol/L) and the concentrations used in fluorescence measurements (2×10^{-4} mol/L M12P5 and 5×10^{-5} mol/L NC12P5 and NC6P5) were used to calculate the effective volume of each polymer aggregate from reorientation time constants found from fluorescence anisotropy measurements. At high polymer concentrations of 0.001 mol/L, the viscosity of each of the three solutions was increased to 1.7 cP for M12P5, 2.8 cP for NC12P5, and 2.5 cP for NC6P5 at 5 °C (see Supporting Information). At the dilute polymer concentrations used in fluorescence measurements, the viscosities of all three polymer solutions were the same as the viscosity of pure water within experimental error.

Steady-State Emission Spectra. Steady-state fluorescence emission spectra were measured for C153 in each of the three polymer solutions and are shown in Figure 7. The emission wavelength of C153 is a sensitive reminder of the polarity of its local environment.[9,35] From a previous study done with coumarins in amphiphilic triblock copolymers, the broadened

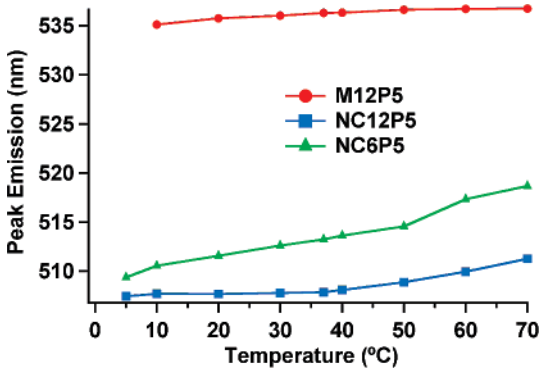

Figure 8. Temperature dependence of steady-state emission peak wavelength of coumarin 153 in M12P5, NC12P5, and NC6P5 aqueous solutions.

line shape results from the coumarin dye experiencing more than one environment and therefore experiencing a distribution of local polarities.[17] The C153 emission maximum is 535 nm for the M12P5 aqueous solution. This peak wavelength indicates that C153 is localized in a polar, water-like environment in the core of the M12P5 micelle.[9,17,35] Although the core is composed of hydrophobic, aliphatic carbons, water is likely present in or near the interior of the micelle. When C153 is solubilized in the cores of each of the two star-like macromolecule aggregates, the emission maximum is 510 nm. This peak wavelength value corresponds to a less polar environment around C153.[9,17,35] The cores of NC12P5 and NC6P5 macromolecule aggregates are more hydrophobic and do not contain polar water molecules to the extent that the core of M12P5 does, according to the fluorescence emission of C153. The peak emission of C153 in both ASM solutions corresponds to a dry core, much like the cores of Pluronic F88 amphiphilic triblock copolymer micelles, as seen in a previous study.[18]

The broad frequency width at half the maximum of the emission spectra of C153 in both NC12P5 and NC6P5 suggests that C153 may be in a range of nonpolar environments within the hydrophobic cores of the two star-like macromolecule aggregates[36] (see Supporting Information for further details of the emission spectral widths).

The peak wavelengths of the C153 emission spectra at 37 °C are shown in Figure 8. The π^* scale is a well-known empirical solvent polarity scale used for a wide variety of common solvents.[37] Values of π^* correlate linearly to the maximum absorption and emission frequencies of C153.[9] As examples of two extremes of the π^* polarity scale, cyclohexane has a π^* of 0.0 and dimethyl sulfoxide has a π^* of 1.00.[9,37] We can compare the local polarity of the C153 probe molecule while encapsulated in the polymeric aggregate using the effective π^* empirical polarity scale discussed by Horng et al.[9] In this way, we can compare the polarity of the molecular probe environment with the values for common organic solvents using the relation $\tilde{\nu}_{em}$ [10^{-3} cm^{-1}] = 21.217 − 3.505π^*. By means of this relationship, the π^* values of the local environment of C153 in M12P5 micelles ranges from 0.72 to 0.74 from 5 to 70 °C. This effective π^* value is similar to the polarity of dichloromethane, which has a value of $\pi^* = 0.73$.[9,37] In NC6P5 and NC12P5 aggregates, the local environment of C153 has π^* values ranging from 0.43 to 0.55 over the same temperature range. The more polar end of this range with $\pi^* = 0.55$ reflects a local polarity similar to THF or benzene.[9,37] The lower end of this range is similar to the polarity of *p*-xylene and ethyl acetate, which both have $\pi^* = 0.45$.[9,37] A plot of the effective π^* vs temperature is given in the Supporting Information. The difference in local

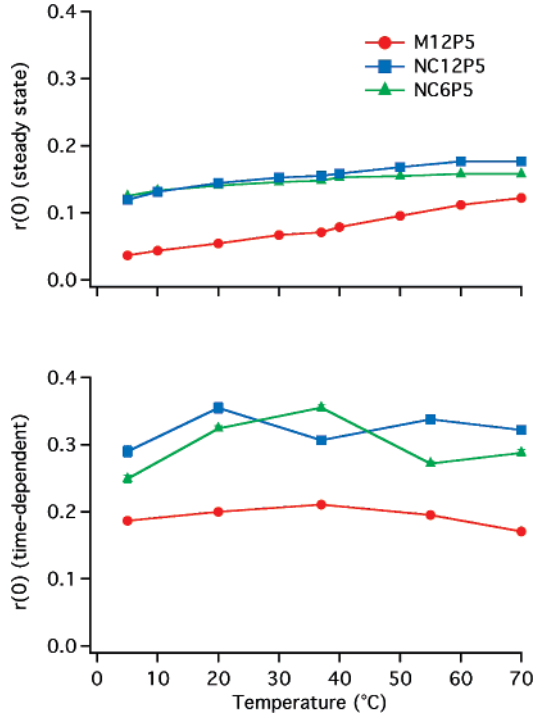

Figure 9. Temperature dependence of the limiting anisotropy from steady-state (top) and time-dependent (bottom) fluorescence depolarization of coumarin 153 in M12P5, NC12P5, and NC6P5 solutions.

polarity between C153 in the ASMs and C153 in the AScM nanocarriers is reminiscent of the shift observed for the $\tilde{\nu}_{em}$ of C153 during aggregation of poly(ethylene oxide)−poly(propylene oxide)−poly(ethylene oxide) triblock copolymers undergoing the unimer-to-micelle nanoscale phase transition.[17] In this case, the local solvation environment of C153 in M12P5 micelles is more polar than the triblock copolymer micelle cores previously studied, and the local environment of C153 in both ASM polymer aggregates is less polar than the presumably "dry" micelle cores.[17]

The temperature dependence of the local polarity of C153 shows that π^* increases slightly with increasing temperature. This rise in polarity is consistent with the rearrangement of ordered water molecules closest to the core of each nanocarrier, causing increased penetration of polar waters toward the hydrophobic core.[38] The emission spectrum of C153 is sensitive to the proximity as well as the electric field of polar water molecules that affect the local solvation polarity around the coumarin dye.[15,16]

C153 Fluorescence Polarization Anisotropies. The fluorescence anisotropy is defined by $r(t) = (I_{VV}(t) - I_{VH}(t))/(I_{VV}(t) + 2I_{VH}(t))$ and is a measure of the amount of depolarization of emitted light due to reorientational motion of the fluorophore.[34] The values of the limiting (or fundamental anisotropy) $r(0)$ range from 0.373 to 0.378 for C153 in a rigid, glassy solvation environment.[17,39] Steady-state anisotropy values were measured with 425 nm excitation and 510 nm emission for the star-like NC12P5 and NC6P5 polymers and at 530 nm for the M12P5 polymer. These values are plotted in Figure 9 (top). The limiting value of the time-dependent anisotropy (eq 7), measured from the TCSPC data, is plotted in Figure 9 (bottom).

$$r(0) = \sum_{j=1}^{n} r_j \qquad (7)$$

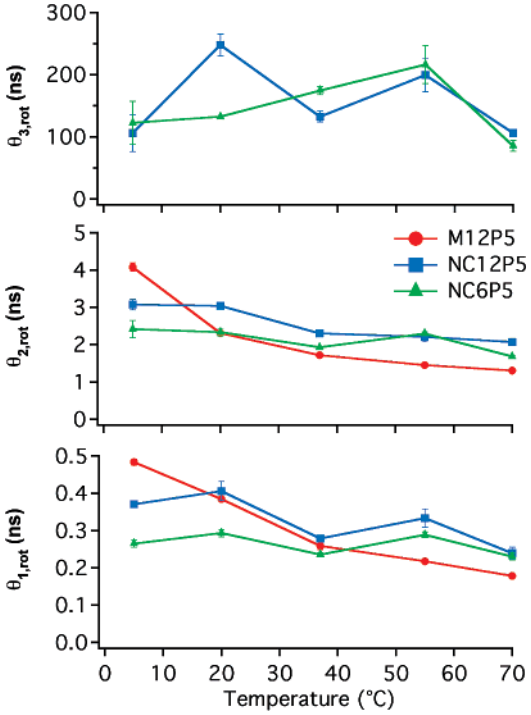

Figure 10. Temperature dependence of reorientation time constants, $\theta_{j,\mathrm{rot}}$'s, for C153 in aqueous solutions of M12P5, NC12P5, and NC6P5.

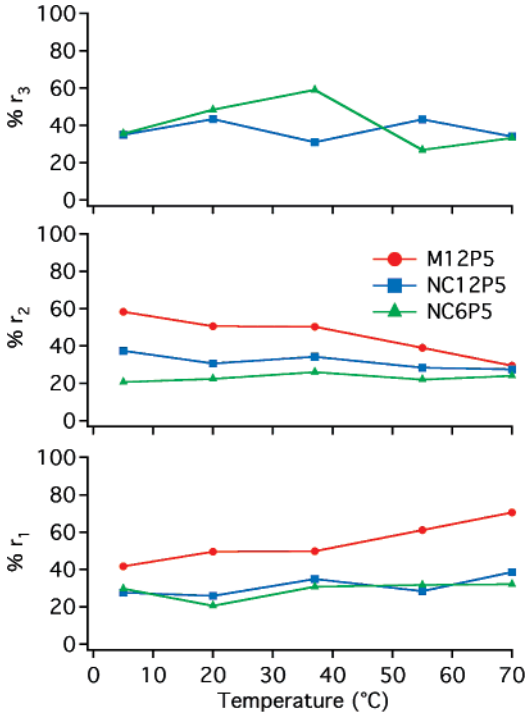

Figure 11. Temperature dependence of percent amplitudes (% r_j of $r(0)$) for C153 time constants in aqueous solutions of M12P5, NC12P5, and NC6P5.

Both the steady-state and time-resolved limiting anisotropies for C153 in M12P5 micelles are lower than those for C153 in the two star-like macromolecule aggregates. The plot of the limiting anisotropy from TCSPC methods vs temperature has the same trend as those values found from steady-state anisotropies. This phenomenon can be attributed to the two star-like macromolecules having a more rigid and hydrophobic core than the scorpion-like polymer micelles. We presume that the AScM micelles are flexible and undergo frequent reorganization and exchange among the monomer constituents, as has been shown

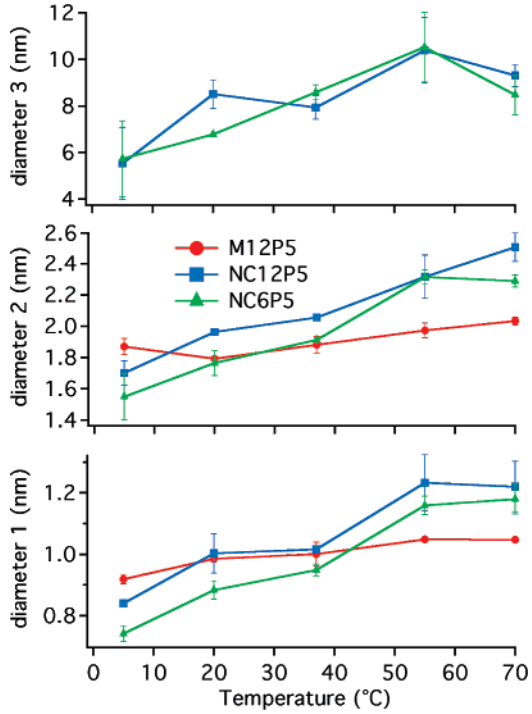

Figure 12. Temperature dependence of effective diameters of C153 reorientation in M12P5, NC12P5, and NC6P5 polymer solutions.

to be the case for a number of other micelle systems.[40−43] Because the cores of ASMs are more rigid, the fluorescence of C153 is not as depolarized as the emission of C153 in the more flexible M12P5 micelle core. The degree of depolarization and, therefore, the fundamental anisotropy, $r(0)$, is dependent on the rotational motion of the fluorophore.[34,44] If the C153 molecule is reorienting relatively rapidly in a water-like environment such as the core of the M12P5 micelle, the emission is more depolarized and $r(0)$ is lower.[34] If C153 is reorienting slowly in a rigid environment, such as the core of a star-like macromolecule aggregate, the degree of depolarization is reduced and $r(0)$ is closer to the theoretical maximum value of 0.4.[34,44]

C153 Fluorescence Dynamics. The time-resolved fluorescence emission decay at 530 nm of C153 in M12P5 was measured over a 70 ns TCSPC time window. The decay transients measured at magic angle polarization were fit to a three-exponential equation. The average fluorescence time constant, $\langle\tau_{\mathrm{fluor}}\rangle$, was calculated using intensity weighting, as expressed in eq 8.[33,34]

$$\langle\tau_{\mathrm{fluor}}\rangle = \sum_{i=1}^{n} \frac{\alpha_i \tau_i^2}{\alpha_i \tau_i} \tag{8}$$

Fluorescence transients for C153 in both NC12P5 and NC6P5 solutions were measured at 510 nm, and these decay transients were fit to a four-exponential equation. The values of $\langle\tau_{\mathrm{fluor}}\rangle$ from 5 to 70 °C for C153 in the M12P5 solution ranged from 4.6 to 4.0 ns. The values of $\langle\tau_{\mathrm{fluor}}\rangle$ from 5 to 70 °C for C153 in the NC12P5 star-like macromolecule aggregate solution ranged from 5.6 to 5.1 ns. The values of $\langle\tau_{\mathrm{fluor}}\rangle$ from 5 to 70 °C for C153 in NC6P5 solution ranged from 5.5 to 4.1 ns.

The solvatochromic behavior of C153 in solvents representing a range of polarities and solvent viscosities is detailed in other articles.[15,16,18] In one previous study,[18] the fluorescence time constant of C153 in a polar (water-PEG) environment was measured and shown to be different than the time constant of

Table 1. C153 Reorientation Time Constants, Associated Fractional Amplitudes, and Anisotropies in Solutions of M12P5, NC12P5, and NC6P5 Ranging from 5 to 70 °C

polymer	$\theta_{1,\mathrm{rot}}$ (ns)	$\theta_{2,\mathrm{rot}}$ (ns)	$\theta_{3,\mathrm{rot}}$ (ns)	r_1	r_2	r_3	$r(0)^a$
M12P5	0.18−0.48	1.30−4.07		0.078−0.120	0.050−0.109		0.171−0.211
NC12P5	0.24−0.41	2.07−3.07	106−248	0.080−0.124	0.088−0.109	0.095−0.154	0.290−0.355
NC6P5	0.23−0.29	1.68−2.42	85.6−216	0.073−0.107	0.060−0.077	0.091−0.181	0.249−0.356

[a] See eq 7.

C153 in a water-free, hydrophobic micelle core environment. In this study of the ABA triblock copolymer Pluronic F88, the fluorescence time constant of C153 was shown to shift from 2.8 ns in a polar, water-like environment to ∼4.6 ns in the hydrophobic, nonpolar core of an ABA triblock copolymer micelle.[18] From the comparison of intensity-weighted average fluorescence time constants of C153 in the three drug delivery polymers in the present discussion, M12P5 micelles show a relatively nonpolar core environment while NC12P5 aggregates have a more extremely nonpolar environment. The fluorescence time constants show that C153 is in a more polar environment in the M12P5 micelle than in the NC12P5 aggregate. The NC6P5 aggregate core polarity, according to C153 lifetimes lies somewhere between the relatively polar M12P5 micelle core and the nonpolar core of the NC12P5 aggregate. This may result because NC6P5 has 96 fewer aliphatic carbons in the core relative to the NC12P5 star-like macromolecule. The fluorescence lifetimes of C153 correlate well with steady-state fluorescence measurements corresponding to local polarity of the fluorescent probe molecule.

Graphs of the fluorescence time constants vs temperature for C153 in aqueous solutions of M12P5, NC12P5, and NC6P5 are available in the Supporting Information, along with plots of the component amplitudes, α_i, time constants, $\tau_{i,\mathrm{fluor}}$, and the intensity-weighted average time constants, $\langle\tau_{\mathrm{fluor}}\rangle$.

C153 Reorientational Dynamics. Drug delivery systems require sequestration and solubilization of hydrophobic drugs as well as the ability to ultimately release the drug. Thus, in successful drug delivery systems, the drug cannot be tightly or chemically bound so as to prevent drug release from the delivery system. We expect that the association characteristics of a drug (or C153 drug model) in ASM aggregates and AScM micelles will display a complex range of orientational dynamics, consistent with the existence of weak association of the drug to multiple sites in the carrier. To investigate the nature of the model drug association with the hydrophobic macromolecular core, we measured the fluorescence depolarization anisotropies of C153.

$$\theta_{\mathrm{rot}} = \frac{V\eta}{k_{\mathrm{B}}T} \tag{9}$$

The Stokes−Einstein−Debye (S−E−D) equation (9) for small reorienting systems relates the reorientation time constant ($\theta_{j,\mathrm{rot}}$) of a fluorescence probe to the effective volume of reorientation (V), the bulk viscosity of the solution (η), and the temperature.[10,26,33,34] The viscosities measured for all polymer solutions were close to that of pure water because the solutions are dilute. Thus, the reorientation time constants give information about the local friction of the fluorophore environment. Reorientational dynamics studied by fluorescence depolarization are relatively uncomplicated for the case of a fluorophore that is rigidly attached to a spherical macromolecule (or nanoparticle). For this case, S−E−D hydrodynamics predictions are often quite accurate. The case of a fluorescence probe that is labile is rather more complex.

The C153 emission decay transients detected at three angles of polarization were concatenated and simultaneously fit to the multiple exponential equations given in eqs 1−5. Best fits yielded three fluorescence time constants and two reorientation time constants for C153 in aqueous M12P5 solution. For C153 in NC12P5 and NC6P5 solutions, best fits yielded four fluorescence time constants and three reorientation time constants. Because the fluorescence anisotropy decay of C153 in each solution has multiple fluorescence and reorientation time constants, we deduce that C153 is in multiple solvation environments within each polymeric nanocarrier.[10,44]

The most significant difference between the two classes of polymers is in the reorientation time constants of C153 between the AScM solution in contrast to ASM solutions. C153 shows a third, longer reorientation time constant in both ASM aggregates, indicating that C153 is moving more slowly, likely experiencing motion with higher local friction in the two ASM solutions than in the more flexible core of the M12P5 micelles. In many cases, it is useful to report the amplitude-weighted average of multiple reorientation time constants.[33,34] In this study, we report all $\theta_{j,\mathrm{rot}}$'s separately, since the long reorientation time constants of C153 in the two ASM solutions greatly dominate such an average and the full range of C153 reorientation time scales would be distorted. Figure 10 shows the individual reorientation time constants of C153 in all three polymers: three in each ASM and two in the AScM solution. Figure 11 shows the percent amplitudes for each reorientation time constant. These data illustrate that each reorientation time constant has a similar contribution to the total reorientation of the fluorophore.

The values of $\theta_{j,\mathrm{rot}}$ and individual anisotropy contributions are listed in Table 1. The two fastest reorientation time constants for C153 in all three polymer solutions are on similar time scales, meaning that the faster motions of the C153 dye are similar in all three nanocarriers. The fastest reorientation time constant ranges from about 0.2 to 0.5 ns, and the second reorientation time constant ranges from about 1.3 to 4.1 ns over the temperature range from 5 to 70 °C. The slowest reorientation time constant, which is only present for C153 in the two ASM aggregate solutions, ranges from approximately 86 to 248 ns.

DLS measurements indicate trimodal particle size distributions for all three polymer solutions; however, the distributions of unimers and large aggregates (>100 nm) are minimal in each case. While the trimodal distribution may affect the distribution of local environments measured, we believe that this is a minimal effect since the hydrophobic C153 will preferentially localize within the more nonpolar micelle or aggregate core that dominates the particle size distribution in all three polymers. We maintain that the C153 and polymer dynamics will remain similar in both aggregate and macroaggregate environments. With this said, we keep in mind that the hydrodynamic volumes of ASM and AScM unimers and aggregates found from DLS are a result of measuring the translational diffusion of these solutions while the hydrodynamic dimensions estimated from the analysis of the TCSPC data result from measuring reorientational diffusion of the coumarin dye. The similarities and

Table 2. Calculated Effective Diameters from C153 Reorientation (Method = C153), Diameters of Polymer Aggregates from DLS (Method = DLS), and Diameters of Unimers from van der Waals Incremental Volumes (Method = vdW) over the Temperature Range from 5 to 70 °C[25,26]

polymer	method	d_1 (nm)	d_2 (nm)	d_3 (nm)	d_{unimer} (nm)
M12P5	C153	0.19−0.33 (±0.01)	1.5−2.4 (±0.05)		
	DLS	5.8−6.7 (±0.8)	9.2−21 (±1.8)	50−340 (±24)	
	vdW				2.11
NC12P5	C153	0.15−0.48 (±0.04)	1.2−3.9 (±0.19)	43−285 (±39)	
	DLS	5.7−5.8 (±0.8)	29−49 (±8)	83−164 (±17)	
	vdW				3.82
NC6P5	C153	0.11−0.43 (±0.02)	0.97−3.3 (±0.09)	49−309 (±44)	
	DLS	2.3−11.1 (±0.2)	26−31 (±5)	53−95 (±14)	
	vdW				3.44

differences that arise in these two methods are displayed in Table 2 (vide infra).

Several possibilities may occur that lead to reorientation time constants that are faster than are predicted by the S−E−D equation (eq 9). The probe may be localized within a region of lower viscosity, such as the water pool in a reverse micelle[44−47] or within a fluid-like micellar core.[17] Another possibility is that the probe is weakly associated with the macromolecule such that there is a more rapid "wobble-in-cone" torsional motion that is sampled by the probe depolarization.[33,34] This effect may be combined with a slower time constant correlated with the overall motion of the macromolecule.

Other possibilities include weak association of the C153 to the polymer. The reorientational dynamics of a probe may show the probe to be rigidly coordinated to the macromolecule and its motion punctuated by bursts of rapid "free" reorientation during brief moments when the probe is unassociated.[34] A case such as this could arise from a probe undergoing sequential release and geminate recombination to the same association site of a macromolecule. Alternatively, a weakly associated fluorescence probe may be sampling a multiplicity of association conformations and/or multiple sites. For any of these cases of weak association to be experimentally observable, association and release must be occurring during the temporal window for fluorescence, which is about 10 times the average fluorescence time constant. The S−E−D hydrodynamics law for molecular reorientation dynamics does not provide information exclusively about the molecular volume of the reorientation species or about the effective local viscosity: rather, S−E−D indicates that time constants obtained by measurement of reorientational dynamics should scale as the product of effective volumes and local viscosities. We consider each limiting case below.

Considering the case of a single, rigid unimer of each macromolecule, θ_{rot} values can be predicted by S−E−D using the estimated incremental van der Waals volume of one unimer and the measured viscosity of each polymer solution.[25,26] These predictions range from 0.5 to 2.2 ns for an M12P5 unimer, 2.5 to 11.6 ns for an NC12P5 unimer, and 1.8 to 8.4 ns for an NC6P5 unimer over the temperature range from 5 to 70 °C. The predicted values for the observed reorientation time constant of unimers are between the second and third time constants of C153 found by TCSPC methods (see Supporting Information).

Effective Diameters for C153 Reorientation. If the C153 were tightly associated with the M12P5, NC6P5, or NC12P5 unimers or aggregates, then each reorientation time constant might be identified with an effective volume (or diameter) for the particles. If this assumption holds true, then this leads to two and three effective volumes of reorientation for M12P5 and for NC6P5 and NC12P5, respectively. The effective diameters derived from these volumes assuming spherical dimensions are plotted in Figure 12. With regard to the fastest motion of C153 measured with time-resolved fluorescence anisotropy, similar reorientation time scales are present in each of the polymer solutions. (For calculated volumes, see Supporting Information.)

The dimensions obtained from this analysis of the C153 fluorescence anisotropy data, assuming S−E−D hydrodynamic behavior, can be compared to the hydrodynamic radii obtained from the DLS data. For the DLS particle size distributions, the smaller diameters obtained are much larger than the diameters inferred from the C153 $\theta_{j,rot}$ values. Applying the methods of Bondi[25] and Edward,[26] the van der Waals volumes for AScM and ASM unimers were estimated to be 5.6 nm^3 for an M12P5 unimer, 29.3 nm^3 for an NC12P5 unimer, and 21.3 nm^3 for an NC6P5 unimer. Assuming that the random-coil polymers are spherical, the corresponding diameters for an M12P5 unimer, an NC12P5 unimer, and an NC6P5 unimer respectively are 2.2, 3.8, and 3.4 nm at 37 °C.

Because the polymers exhibit flexible random coil behavior in solution, the fastest reorientation time constants, $\theta_{1,rot}$ from C153 fluorescence represent a smaller volume and a faster motion than the reorientation of an entire unimer for each of the three polymers. These time constants range from 0.2 to 0.5 ns and are assigned to hindered orientational diffusion of C153 molecules loosely associated with the ASM or AScM polymers. The corresponding diameters are therefore in the range 0.2−0.5 nm, approximately the diameter of the coumarin molecule itself.

Assuming that the bulk viscosity also is an accurate measure of the local friction, the second reorientation time constants $\theta_{2,rot}$ correlate to slightly larger effective volumes in all three polymer solutions. For C153 in M12P5 solution, $\theta_{2,rot}$ correlates well with the volume of a unimer having a diameter of 2.2 nm. The effective diameters obtained from C153 reorientation in the second mode are on the order of 1.5−3.9 nm, approximately the same dimensions of each polymeric unimer according to incremental van der Waals molecular volumes.[25]

The third reorientation time constant $\theta_{3,rot}$ for C153 in the two ASM polymer solutions corresponds to effective diameters larger than a single ASM unimer and approximately the same or slightly larger than the dominant aggregate sizes indicated by DLS. For NC12P5, the range of diameters predicted from C153 reorientational dynamics is 43−285 nm. Likewise, the range of diameters deduced from C153 fluorescence anisotropy in NC6P5 solution is from 49 to 309 nm. The existence of the third, longer reorientation time constant, $\theta_{3,rot}$, in the two ASM polymer solutions further indicates that aggregation is occurring and that C153 is experiencing local reorientation on a size scale close to that of an aggregate. A comparison of the predicted diameters for each of the polymers in solution is presented in Table 2.

Microviscosity in ASM and AScM Cores. The Stokes−Einstein−Debye (S−E−D) equation has shown to be quite useful for correlating the viscosity, temperature, and molecular volume of the reorienting species with the orientational correlation time constant for aqueous and organic solvent solutions.[10,33,34] The local friction actually experienced by a molecular probe is often poorly correlated to the bulk solution

Table 3. Calculated Local Frictions of C153 in Each Aqueous Polymer Solution from Individual Reorientation Time Constants[10]

polymer	$\eta_{local,1}$ (cP)	$\eta_{local,2}$ (cP)	$\eta_{local,3}$ (cP)
M12P5	3.2−9.1	26−84	
NC12P5	4.4−7.6	41−63	2500−6050
NC6P5	4.2−5.4	33−49	2000−5250

viscosity. In polymer solutions, the S−E−D equation is applied in a different way than for the simpler case of organic solvents. Horng et al. have derived an empirical equation for obtaining the effective solvent viscosity from the measured reorientational time constants obtained from C153 fluorescence anisotropy experiments.[10] Their equation $\langle\theta_{rot}\rangle_{polar} = (58.1 \pm 1.6)\eta^{0.96\pm0.03}$ holds for a wide range of polar organic solvent environments.[10] We have shown above that the effective polarity of these environments ranges from about 0.4 to 0.7 on the π^* empirical solvent polarity scale, which shows that our C153 probe is always experiencing a moderately polar environment.

One interpretation of the multiple exponential orientational time constants that we observe for C153 in the ASM and AScM solutions is that the C153 is distributed heterogeneously among sites with different microviscosities. Making this assumption, we can predict the effective microviscosity experienced by the C153 using the equation of Horng et al. above.[10] The results from applying this equation are presented in Table 3. The fastest reorientation time constants lead to microviscosity values η_1 in the 3.2−9.1 cP range, consistent with weak entanglement in a hydrophilic polymer solution. The second time constants lead to predicted microviscosities η_2 in the range from 26 to 84 cP. Only in the ASM aggregates, NC6P5 and NC12P5, are the higher friction values observed. For these solutions, the third reorientational time constant can be used to predict a microviscosity ranging from 2500 to 6050 cP. These values are larger than we observed in the micellar cores of PEO−PPO−PEO triblock copolymer model systems, for which the maximum microviscosity of 890 cP was found for a bcc lattice hydrogel solution of micelles.[17] The measured bulk viscosities of the aqueous polymer solutions are available in the Supporting Information and range from 0.4 to 1.6 cP. The local friction of C153 experienced in these polymer solutions is much larger than the bulk solution viscosity for all solutions and temperatures measured. The difference in local friction of C153 between the three polymers is a further indication that C153 is more rigidly encapsulated inside the two amphiphilic star-like macromolecule aggregates than in the scorpion-like M12P5 micelle.

Summary and Conclusions

The fluorescent coumarin 153 dye was solubilized in three amphiphilic polymers that were designed and synthesized for the purpose of hydrophobic drug encapsulation. Steady-state and time-resolved fluorescence studies of C153 in each solution were performed over a range of temperatures from 5 to 70 °C to reflect encapsulation behavior at several temperatures. Analysis of the steady-state emission shows that C153 is in a polar environment in the AScM polymer solution and in a less polar environment in the two ASM polymers. Dynamic light scattering measurements provide insight into the aggregation of both ASM and AScM polymers. DLS results show aggregates in solution with a distribution of sizes from 10 to 40 nm, which is well under the 100 nm limit for good bioavailability.[1,2] Hydrodynamic radii obtained from analysis of DLS data were compared to those deduced from C153 polarization anisotropy as well as estimated unimer diameters found from incremental van der Waals volumes.[25,26] From shear viscosity measurements, the bulk viscosity of these solutions is close to that of bulk water,[48] while the local friction as reported by C153 in solutions of ASM and AScM aggregates is substantially higher for each of three orientational motions of C153 detected.

Analysis of time-resolved fluorescence anisotropy measurements yielded multiple rates of fluorescence and multiple reorientation time constants for C153 in each of the polymer aggregate local environments. The fluorescence lifetimes do not reflect any nanoscale phase changes such as micellization or demicellization at the polymer concentrations studied but indicate that the C153 probe is in a more polar core environment in the M12P5 micelle than in the NC12P5 star-like macromolecule aggregate. The lifetimes also show that the core of the NC6P5 aggregate has an intermediate polarity in comparison to the other two nanocarriers.

It is likely is that C153 is experiencing multiple solvation sites within polymer aggregates. Though unimers are likely to be diffusing in and out of different aggregates, C153 seems to localize in the covalently bonded core of each polymer, near the hydrocarbon chains at each acylated mucic acid region, or at the interface between the hydrocarbon core and the PEG corona of each nanocarrier.

In comparing the ASMs and AScMs, the individual reorientation time constants found from polarization anisotropy measurements show that C153 is more rigidly associated with the nonpolar core of each ASM polymer and in a more polar environment in the flexible core of the AScM micelle. The effective diameters from C153 reorientation applying S−E−D hydrodynamics correlate to multiple reorientational motions of C153 in both ASMs and AScM solutions. These data support the conclusion that C153 is solvated in multiple regions inside the core of each polymeric nanocarrier. The longer reorientation time constants of C153 in NC12P5 and NC6P5 polymers are evidence that C153 is rigidly solvated in the core of the star-like nanocarriers, while the dye is loosely solvated in the polar core of the AScM micelles.

These C153 fluorescence studies provide the details of the local polarity and microviscosity within the encapsulated sites of the ASM and AScM polymer aggregates and micelles, respectively. If an encapsulated drug requires increased solubility, but a longer retention profile, the more hydrophobic, rigid core of the two ASM aggregates may be more useful than the flexible core of AScM micelles. The local drug solvation properties of future derivatives of these and most other polymeric macromolecules can be methodically characterized using the methods described in this study.

Acknowledgment. We gratefully acknowledge financial support from the National Science Foundation (NSF-CHE-0239390). Karen Steege gratefully acknowledges support as a Rutgers University NSF-IGERT Fellow (NSF DGE-0333196). Jinzhong Wang gratefully acknowledges support from the American Heart Association. We thank Benjamin Lee, Jason Giurleo, Jeremy Pronchik, Troy Messina, and Prof. David Talaga for contributions to Igor Pro anisotropy fitting code. We also thank Prof. Lawrence Romsted for use of the Nicomp particle sizing system.

Supporting Information Available: Volume-weighted particle size distributions are presented as concentration and temperature-dependent data from DLS measurements; shear viscosity values at various temperatures are presented for two concentrations of each bulk polymer solution; broad spectral line widths of steady-state emission spectra of C153 in each drug delivery polymer solution are presented as fwhm values vs sample temperature; calculated from steady-state emission peak wavelengths, π^* polarity values

are presented for the local environment of C153 in each polymer solution; fluorescence time constants of C153 are presented as intensity-weighted average as well as individually for all three polymers; from the estimated van der Waals volumes of single ASM and AScM unimers, θ_{rot} can be predicted from S−E−D hydrodynamics, and these predicted values are presented for a range of sample temperatures; from the C153 reorientation time constants measured with TCSPC, the effective volumes of C153 reorientation are calculated with eq 9 and presented with changing temperature; from Horng et al., the local friction of C153 is calculated for polar solvation from $\theta_{j,rot}$ values and are presented graphically. This material is available free of charge via the Internet at http://pubs.acs.org.

References and Notes

(1) Duncan, R. *Nat. Rev. Drug Discovery* **2003**, *2*, 347−360.
(2) Kwon, G. S. *Crit. Rev. Ther. Drug Carrier Syst.* **2003**, *20*, 357−403.
(3) Krsko, P.; Libera, M. *Mater. Today* **2005**, *8*, 36−44.
(4) Khandare, J.; Minko, T. *Prog. Polym. Sci.* **2006**, *31*, 359−397.
(5) Harris, J. M., Zalipsky, S., Eds. *Poly (ethylene glycol): Chemistry and Biological Applications*; ACS Symposium Series 680; American Chemical Society: Washington, DC, 1997; pp 1−12.
(6) Miao, J.; Xu, G.; Zhu, L.; Tian, L.; Uhrich, K. E.; Avila-Orta, C. A.; Hsiao, B. S.; Utz, M. *Macromolecules* **2005**, *38*, 7074−7082.
(7) Xing, L.; Mattice, W. L. *Macromolecules* **1997**, *30*, 1711−1717.
(8) Kwon, G. S.; Forrest, M. L. *Drug Dev. Res.* **2006**, *67*, 15−22.
(9) Horng, M. L.; Gardecki, J. A.; Papazyan, A.; Maroncelli, M. *J. Phys. Chem.* **1995**, *99*, 17311−17337.
(10) Horng, M. L.; Gardecki, J. A.; Maroncelli, M. *J. Phys. Chem. A* **1997**, *101*, 1030−1047.
(11) Cave, R. J.; Castner, E. W., Jr. *J. Phys. Chem. A* **2002**, *106*, 12117−12123.
(12) Ingrosso, F.; Ladanyi, B. M.; Mennucci, B.; Scalmani, G. *J. Phys. Chem. B* **2006**, *110*, 4953−4962.
(13) Ingrosso, F.; Ladanyi, B. M. *J. Phys. Chem. B* **2006**, *110*, 10120−10129.
(14) *ChemDraw Ultra 10*, CambridgeSoft, Cambridge, MA, 2005.
(15) Reynolds, L.; Gardecki, J. A.; Frankland, S. J. V.; Horng, M. L.; Maroncelli, M. *J. Phys. Chem.* **1996**, *100*, 10337−10354.
(16) Jones, G. G., II; Jackson, W. R.; Choi, C. Y.; Bergmark, W. R. *J. Phys. Chem.* **1985**, *89*, 294−300.
(17) Grant, C. D.; Steege, K. E.; Bunagan, M. R.; Castner, E. W., Jr. *J. Phys. Chem. B* **2005**, *109*, 22273−22284.
(18) Grant, C. D.; DeRitter, M. R.; Steege, K. E.; Fadeeva, T. A.; Castner, E. W., Jr. *Langmuir* **2005**, *21*, 1745−1752.
(19) Frauchiger, L.; Shirota, H.; Uhrich, K. E.; Castner, E. W., Jr. *J. Phys. Chem. B* **2002**, *106*, 7463−7468.
(20) Tian, L.; Yam, L.; Zhou, N.; Tat, H.; Uhrich, K. E. *Macromolecules* **2004**, *37*, 538−543.
(21) Tian, L.; Yam, L.; Wang, J.; Tat, H.; Uhrich, K. E. *J. Mater. Chem.* **2004**, *14*, 2317−2324.
(22) Liu, H.; Jiang, A.; Guo, J.; Uhrich, K. E. *J. Polym. Sci., Part A: Polym. Chem.* **1999**, *37*, 703−711.
(23) Tao, L.; Uhrich, K. E. *J. Colloid Interface Sci.* **2006**, *298*, 102−110.
(24) Djordjevic, J.; Barch, M.; Uhrich, K. E. *Pharm. Res.* **2005**, *22*, 24−32.
(25) Bondi, A. *J. Phys. Chem.* **1964**, *68*, 441−451.
(26) Edward, J. T. *J. Chem. Educ.* **1970**, *47*, 261−270.
(27) Ben-Amotz, D.; Drake, J. M. *J. Chem. Phys.* **1988**, *89*, 1019−1029.
(28) *Igor Pro 5.04b Edition*, Wavemetrics, Inc., Lake Oswego, OR, 2005.
(29) Sun, Y.; Castner, E. W., Jr.; Lawson, C. L.; Falkowski, P. G. *FEBS Lett.* **2004**, *570*, 175−183.
(30) Shirota, H.; Castner, E. W., Jr. *J. Chem. Phys.* **2000**, *112*, 2367−2376.
(31) Becker, W. *Advanced Time-Correlated Single Photon Counting Techniques*; Springer: New York, 2005; pp 61−82.
(32) Cross, J. A.; Fleming, G. *Biophys. J.* **1984**, *46*, 45−56.
(33) Lakowicz, J. R. *Principles of Fluorescence Spectroscopy*, 2nd ed.; Kluwer Academic/Plenum Publishers: New York, 1999; pp 129−131, 304−305, 322−329.
(34) Valeur, B. *Molecular Fluorescence: Principles and Applications*; Wiley-VCH: New York, 2002; pp 130−131, 136−139, 145−147, 172−173, 243.
(35) Maroncelli, M.; Fleming, G. R. *J. Chem. Phys.* **1987**, *86*, 6221−6239.
(36) Matyushov, D. V.; Newton, M. D. *J. Phys. Chem. A* **2001**, *105*, 8516−8532.
(37) Kamlet, M. J.; Abboud, J. L.; Taft, R. W. *J. Am. Chem. Soc.* **1977**, *99*, 6027−6038.
(38) Bhattacharyya, K.; Bagchi, B. *J. Phys. Chem. A* **2000**, *104*, 10603−10613.
(39) Gardecki, J. A.; Maroncelli, M. *Chem. Phys. Lett.* **1999**, *301*, 571−578.
(40) Halperin, A.; Alexander, S. *Macromolecules* **1989**, *22*, 2403−2412.
(41) Michels, B.; Waton, G.; Zana, R. *Langmuir* **1997**, *13*, 3111−3118.
(42) Mays, H.; Almgren, M. *J. Phys. Chem. B* **1999**, *103*, 9432−9441.
(43) Lund, R.; Willner, L.; Stellbrink, J.; Lindner, P.; Richter, D. *Phys. Rev. Lett.* **2006**, *96*, 068302.
(44) Bialik, C. N.; Wolf, B.; Rachofsky, E. L.; Ross, B. A.; Laws, W. R. *Biophys. J.* **1998**, *75*, 2564−2573.
(45) Levinger, N. E. *Curr. Opin. Colloid Interface Sci.* **2000**, *5*, 118−124.
(46) Pant, D.; Levinger, N. E. *Langmuir* **2000**, *16*, 10123−10130.
(47) Harpham, M. R.; Ladanyi, B. M.; Levinger, N. E.; Herwig, K. W. *J. Chem. Phys.* **2004**, *121*, 7855−7868.
(48) Weast, R. C., Astle, M. J., Eds.; *CRC Handbook of Chemistry and Physics*, 61st ed.; CRC Press: Cleveland, OH, 1980; p F-51 .

MA061779L